Proceedings of OMAE'2001
2001 ASME Offshore Mechanics and Arctic Engineering
June 03–08, 2001, Rio de Janeiro, RJ, Brazil

OMAE01/OFT-1264

COLLAPSE ANALYSIS OF STIFFENED PANELS DURING ACCIDENTAL CONDITIONS

Abuu K. Mohammed*
Marine Structures Dept., NTNU
Email: abhali@marin.ntnu.no

Jørgen Amdahl
Marine Structures Dept., NTNU
jamda@marin.ntnu.no

Bjørn Skallerud
Applied Mechanics Dept., NTNU
bjorn.skallerud@mtf.ntnu.no

Norwegian University of Science and Technology (NTNU)
N-7491 Trondheim
NORWAY

ABSTRACT

The performance of a non–linear elasto–plastic formulation based on triangular shell finite elements is tested against several practical applications. The analyses include buckling of stiffened plates under combined axial compression and lateral pressure, shear collapse of thin–walled aluminum plate girder, and an axial crushing of a cruciform (X–element). The simulations are compared with other finite elements, experimental results, and design codes. For stiffened plates, comparison with DnV Classification notes shows that the latter becomes non–conservative with higher pressure loads. For the plate girder and X–element, fine agreement of the deformations between the simulations and experimental results is observed.

INTRODUCTION

During accidental conditions — such as collision, grounding, explosions, and fires — ships and offshore structures are subjected to extreme loads. Contrary to the conventional ultimate strength designs, system effects should be taken into account during such events. In other words, local collapse is accepted provided that global integrity is not put into jeopardy. If such effects are to be considered in a non–linear finite element analysis, efficient computational algorithms are required.

The objective of the present work is to find simple formulations that can be applied to predict the ultimate strength of stiffened panels. In this context, non–linear shell finite elements and material plasticity will be the main focus for the ultimate strength or collapse analyses of stiffened panels subjected to extreme loads.

The goal is to implement these formulations in the computer program USFOS (1998), which was originally developed for progressive collapse analyses of offshore structures based on space–frame representation. With the implementation of non–linear shell finite elements, refined modeling in areas with large inelastic deformations is made possible while the rest of the structure can remain as beam elements.

The theory of the present formulation has been presented earlier by the authors (see Mohammed *et al*. (2000)). In the present paper, the numerical tool is verified for various practical applications. The analyses include stiffened plates subjected to axial compression, plate girder subjected to shear loading, and axial crushing of a cruciform. The latter is commonly known as X–element in the context of ship collision and grounding mechanics.

The formulation that is verified in this paper is based on a triangular constant stress–resultants shell finite element belonging to the family of Morley elements (Morley (1971)). The element has twelve degrees–of–freedom including three displacement at each of the corner nodes and one rotation at each of the mid–side nodes. The material formulation is based on stress–resultants plasticity with one integration point in the element plane. It involves a solution of a single scalar equation for the plasticity mul-

*Address all correspondence to this author

Copyright © 2001 by ASME

tiplier (see Mohammed *et al.* (2000) for detailed derivations).

In USFOS (1998), the present shell will be another alternative to the implementation of Skallerud and Haugen (1999), which is already in place, for three and four node facet elements. The existing implementation uses the same plasticity formulation with a number of integration points along the element's plane.

The paper starts with buckling analyses of steel stiffened plates. The simulations are compared with the results from another finite element program ABAQUS (1998) and the predictions from DnV (1992) design code. Thereafter, an example of aluminum plate girder collapsing under shear loading is presented. For this part, the results are compared with the experiments and the predictions from Eurocode-9 (1998). Finally, crushing analysis of an X–element collapsing under axial force is presented. The results are compared with the analytical values from a simplified model.

STIFFENED PLATE PANELS

In ship structural design, one of the major consideration is the ultimate strength of the hull girder. Generally, it is accepted that this strength can be represented by the strength of the representative longitudinally stiffened panels. The panels include plate panels, longitudinal stiffeners, and transverse frames as illustrated in Figure 1. The load–shortening curves of these panels can be utilized to predict the overall ultimate strength.

For panels in compression, the basic forces are the axial compression from the overall hull girder bending moment, local bending from lateral pressure, transverse compression from the in–plane pressure loads, and the shear forces. Most of the classification societies recommend a beam–column approach for design. In this approach, a single longitudinal stiffener with the associated plate flange is considered representative for the behaviour of the longitudinally stiffened panel.

At the time of testing the present formulations, it was possible to analyze only a combination of axial compression and lateral pressure loads.

Reference Stiffened Plates

Nine T–stiffened plates taken between two transverse frames were analyzed. The scantlings are given in Table 1, from which $\bar{\lambda}$ is the reduced slenderness ratio and β is the plate slenderness. They are defined as,

$$\bar{\lambda}^2 = \frac{\sigma_Y}{\sigma_E}, \qquad \beta = \frac{b_p}{t_p}\sqrt{\frac{\sigma_Y}{E}} \tag{1}$$

where σ_Y is the yield stress, σ_E is the Euler buckling stress, and E is the Young's modulus. The geometrical parameters are described in Figure 2.

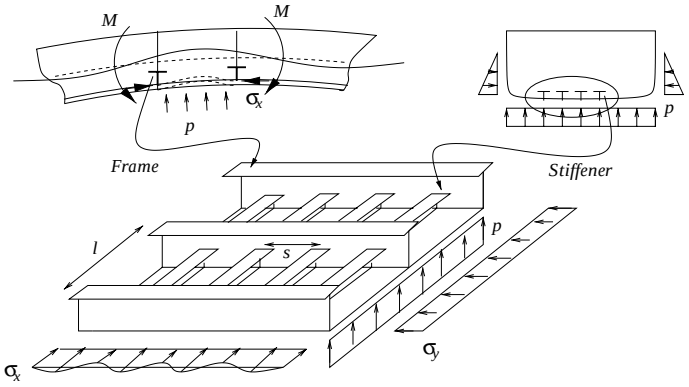

Figure 1. SHIP HULL GIRDER

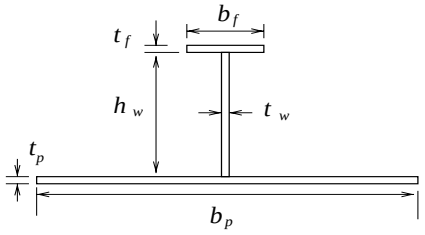

Figure 2. CROSS–SECTION OF THE STIFFENED PLATE

Table 1. GEOMETRICAL PARAMETERS

$\bar{\lambda}$	β	$t_p[mm]$	$h_w[mm]$	$t_w[mm]$	$b_f[mm]$	$t_f[mm]$
0.19	1.64	23.00	300	15.0	100	24.0
	2.19	17.25	300	10.0	100	16.0
	2.74	13.80	300	10.0	100	11.2
0.32	1.64	23.00	200	11.0	100	17.0
	2.19	17.25	200	9.0	100	10.8
	2.74	13.80	200	6.0	100	7.8
0.51	1.64	23.00	120	12.0	100	17.0
	2.19	17.25	120	9.0	100	11.8
	2.74	13.80	120	6.0	100	8.7

Within the panel, the transverse frame spacing was taken to be $l = 3000$mm while the longitudinal stiffener spacing was $s = b_p = 1000$mm. The steel material was assumed to be elastic–perfectly–plastic with $E = 2.1 \times 10^5$ MPa, $\sigma_Y = 300$ MPa, and $\nu = 0.3$.

Copyright © 2001 by ASME

Finite Element Modeling

The finite element mesh for the reference panel is as shown in Figure 3. Depending on the height of the web, each model consists of 1920–2240 triangular shell elements. This mesh can be considered to be very fine. It is therefore important to point out that the same reasonable solution could be reached with a much coarser mesh. However, based on the regular mesh generator available and the modeling style used, this mesh was found to be the best choice.

Fixed (clamped) boundary conditions were imposed at the panel ends. The axial boundary conditions on one of the panel end was modeled in such a way as to give uniform axial displacements. Along the longer edges of the main plating, symmetric boundary conditions were imposed.

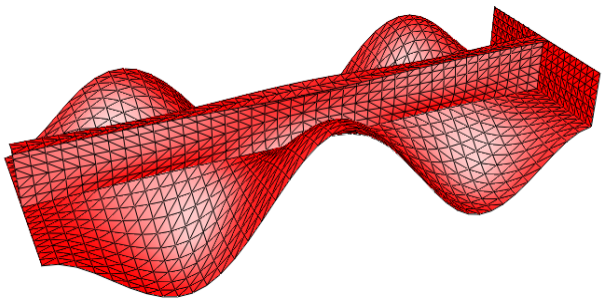

Figure 3. THE REFERENCE PANEL; MESH AND PLATE IMPERFECTION

Initial Imperfections. In a non–linear finite element analysis of welded structures, it is generally necessary to introduce initial imperfections so as to obtain results which represent the practical conditions. The imperfections are aimed to model the effects of true initial distortions, residual stresses due to fabrications, imperfect geometry, etc. The magnitude of these imperfections are not known. Normally, they are either selected so as satisfy the tolerance requirements, or calibrated so that the buckling design curves are reproduced. Often, these two procedures yield approximately the same results.

In the present analyses, three types of initial imperfections were considered with the maximum allowable tolerance based on the DnV design code. These imperfections include mainly two sources: plate out–of–plane displacements (w_p), and stiffener out–of–straightness relative to the plate plane (w_s). The latter will be referred to as stiffener beam imperfection.

For the plate imperfection, a quadratic sinusoidal function is the natural choice. From a linearized buckling analysis, the buckling pattern can be selected as depicted in Figure 3, where the displacements are magnified 35 times for clarity. This pattern can be considered to represent the shape of plate imperfection.

As it can be seen from Figure 3, if the plate imperfection is to be considered, a third type of imperfection is added naturally. This is due to the stiffener out–of–plane displacements which are the results of plate rotations. Because of the T–stiffener in the present analyses, this type of imperfection is very small, however it was retained.

The maximum allowable value for plate imperfection was set at $w_p^\circ = 10$mm according to DnV code. A single sinusoidal wave was taken as the stiffener beam imperfection with the maximum allowable value set at $w_s^\circ = 4.5$mm.

Ultimate Strength Analyses

Anticipating plate induced failure and a symmetric buckling mode, the lateral pressure was applied on the plate side throughout the analyses. Together with the axial forces, the loading was incremented proportionally until collapse. The basic idea for simultaneous increments is that the ultimate capacity will be reached earlier than when the pressure is applied to a fixed unit factor. Similar approach was used to obtain the predictions from the DnV design code.

The load–shortening curves are shown in Figures 4–6. In these curves, the results from ABAQUS are presented as well. It is observed that there is a good agreement between the two simulations. A typical panel after failure is shown in Figure 7.

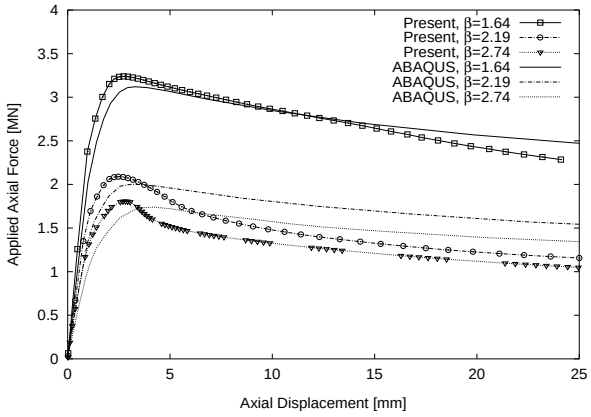

Figure 4. LOAD–SHORTENING CURVES FOR $\bar{\lambda} = 0.19$

Though the results from both finite element formulations show a good agreement, a deviation of up to 30% is observed for stiff panels with $\bar{\lambda} = 0.19$ when comparison with DnV (1992) is made. This is depicted in Figure 8 in terms of critical stress versus plate slenderness.

As regard to critical failure mode, however, the DnV design code was in agreement with the finite element simulations. For instance, in panels with $\bar{\lambda} = 0.19$, the present finite element for-

Copyright © 2001 by ASME

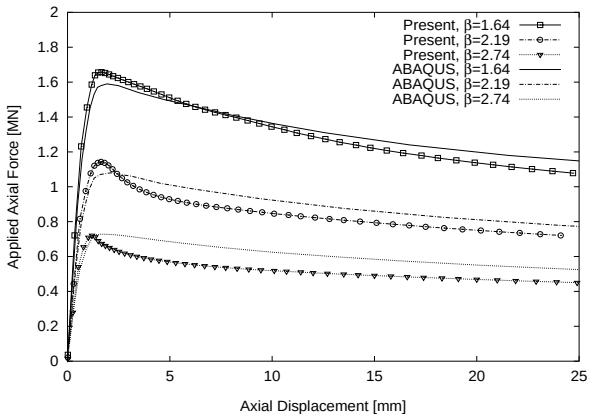

Figure 5. LOAD–SHORTENING CURVES FOR $\bar{\lambda} = 0.32$

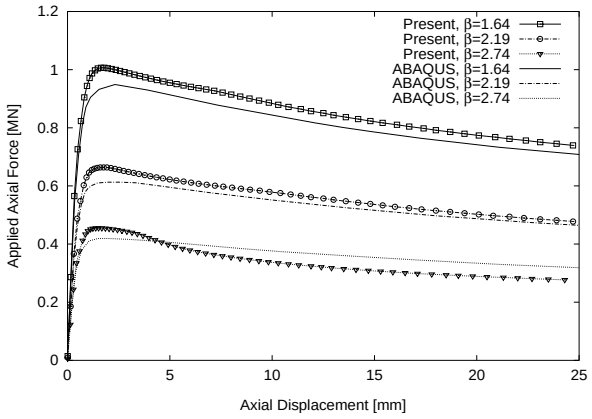

Figure 6. LOAD–SHORTENING CURVES FOR $\bar{\lambda} = 0.54$

mulation showed that they were failing with plate induced compressive failure. On the other hand, for $\bar{\lambda} = 0.32$ and $\bar{\lambda} = 0.51$, tensile yielding of the stiffener was the governing mode. Similar predictions are made by the DnV design code.

The Effect of Lateral Pressure. To evaluate the DnV design code for the observed deviation in ultimate capacity with respect to stiff panels, a panel with $\bar{\lambda} = 0.19$ and $\beta = 2.19$ was selected for further investigation.

Since it is clear that with proportional load increments stiff panels carry large pressure loads as well, it was found interesting to vary the magnitude of applied reference pressure load. In doing so, the load–shortening curves were obtained as shown in Figure 9. As expected, the ultimate capacity increases with decreasing reference lateral pressure.

The plots of critical axial stress versus critical pressure load in Figure 10 indicates that: while the DnV code is very conservative for lower pressure loads, it becomes non–conservative with higher lateral pressure loading. Similar observation can also be made clearly in the results presented by Wang and Moan (1997) where a combined bi–axial and lateral pressure loads were applied to stiffened plates with L–type stiffeners. In the latter, the lateral pressure was applied only to a fixed level, while the axial compression was incremented until collapse.

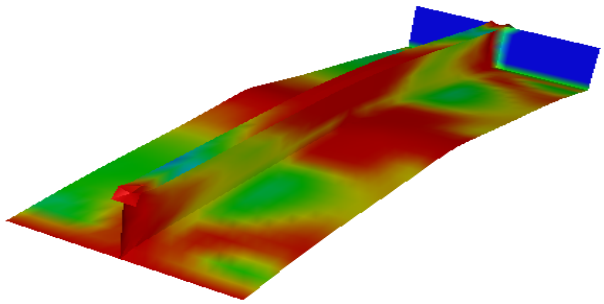

Figure 7. STRESS DISTRIBUTION AFTER COLLAPSE

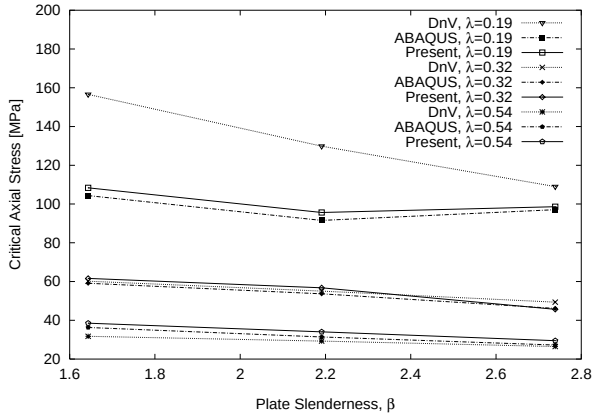

Figure 8. CRITICAL STRESS W.R.T. SLENDERNESS

SHEAR COLLAPSE OF ALUMINUM PLATE GIRDER

Generally, design criteria for plate girders without longitudinal stiffeners involve checking of bending and shear stresses as well as the local and overall instabilities. For plates in shear, an important component of post collapse strength may result from the diagonal tension that develops. This effect is commonly known as the tension field action, and it depends on the relative flexibility between the girder components.

For girders with thin webs and strong flanges, very high capacity in shear is obtained with the web plate resisting much of the applied load in tension. This effect has been studied for many decades. The basic theoretical background and references can

Copyright © 2001 by ASME

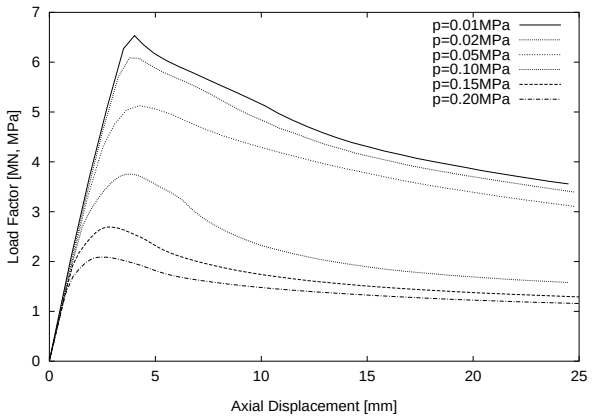

Figure 9. LOAD–SHORTENING CURVES FOR DIFFERENT REFERENCE PRESSURE LOADS; REFERENCE AXIAL FORCE = 1MN

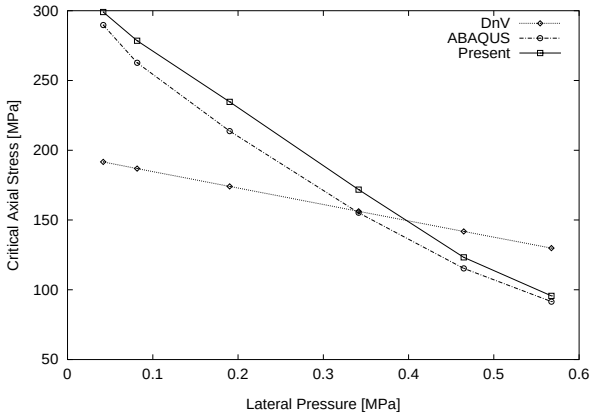

Figure 10. THE INFLUENCE OF LATERAL PRESSURE

be found in ECCS (1986). In the work of Höglund (1997), the design method and summary on a number of experimental results reported in the literature on aluminum alloy and steel plate girders are presented. For shear buckling resistance according to Eurocode-9 (1998), this method is the basis.

The analyses in this section are based on the work of Langhelle and Eberg (1999) who carried out a series of tests on aluminum plate girder under different temperatures. Here we shall focus only on the test results at room temperature. The scantlings of the tested girder, which is an end panel, are shown in Figure 11. In end panels, the dominating force is the shear including horizontal forces from the inner panels. In thin webs, this shear capacity depends on whether the end post is stiff or weak in the longitudinal girder. According to Eurocode-9 (1998), the relative dimensions of this girder satisfy the condition of having a rigid end post.

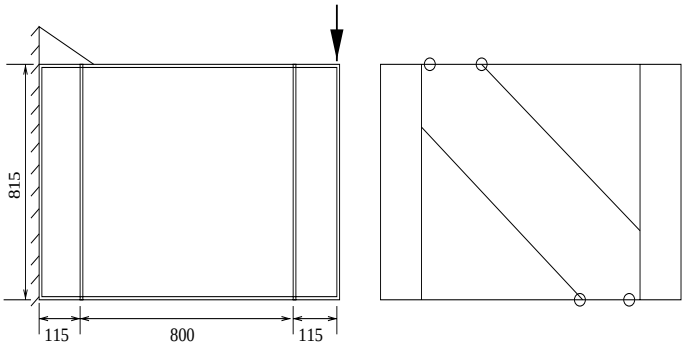

Figure 11. ALUMINUM PANEL; SCANTLINGS

Finite Element Analyses

The finite element modeling considered a clamped boundary condition on one end. At the remaining end, out–of–plane web displacements were restricted. A concentrated shear force equal to 1000KN was applied at the free end. A similar modeling was applied in ABAQUS analyses.

The load–displacement curves from the analyses and tests are shown in Figure 12 along with Eurocode-9 (1998) predictions. In general, the finite elements and test results correspond well. The slight deviations observed can be attributed to the uncertainties of nominal material properties. The results of the two finite element formulations are very close to each other, which shows that the present finite element formulation performs equally well with the more detailed formulations. It should be noted that ABAQUS uses a number of integration points through thickness and plane, while the present formulation considers a single integration point per element.

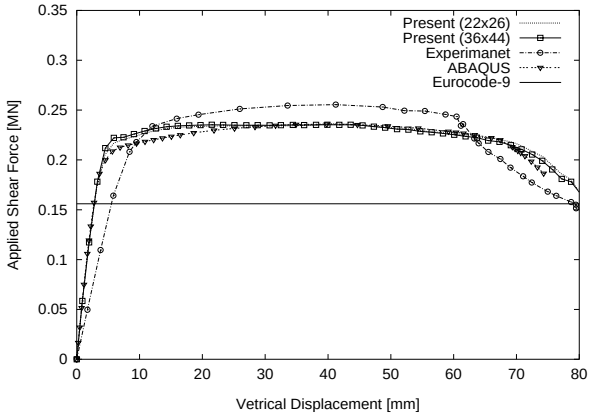

Figure 12. LOAD–DISPLACEMENTS CURVES FOR ALUMINUM PLATE GIRDER

Copyright © 2001 by ASME

(a) Test; Langhelle and Eberg (1999) (b) Simulation

Figure 13. ALUMINUM PLATE GIRDER

From Figure 12, it is seen that the predictions from Eurocode-9 (1998) design code for shear buckling resistance of plate girders are very conservative.

Figure 13 shows the girder picture after collapse. It is seen that the finite element analysis has captured the displacement pattern in the test, very well.

CRUSHING STRENGTH OF A CRUCIFORM

In the field of crashworthiness, the crushing response of ship panels is of primary importance for a reliable engineering analysis. Usually, the response involves large deformations of shells and local instabilities, followed by localization of plastic deformations. Detailed analysis may often be prohibitive in terms of computer time and storage, and therefore a need for simplified modeling procedure becomes an alternative. Such models are given e.g. by Amdahl (1983). The procedure is based on dividing the structure into basic elements such as X, Y, and T–elements instead of plane plate or shell elements. The idea is that the material in the immediate vicinity of a plate intersection absorbs most of the energy.

Analytical Method

The analytical prediction of energy absorption in a structure during crushing is based on a simplified energy method. In this approach the external work must balance the internal energy stored or dissipated in the structure. The analytical models such as Amdahl (1983) and Kierkegaard (1993) assume complete ductility with no material fracture.

Based on experimental work on X and T–elements made from steel material, it is suggested that the structure is crushed with an intersection line between the flanges remaining straight (see Figure 14). This failure mode is commonly referred to as the straight edge mechanism. The basic folding mechanism is presented by Amdahl (1983).

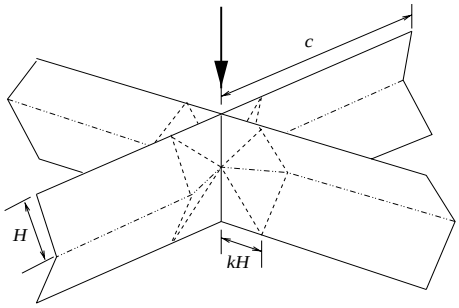

Figure 14. A CRUCIFORM; STRAIGHT EDGE MECHANISM

The X–element can be considered more representative since the average crushing force for the remaining basic elements can be deducted from it. For the cruciform element the average crushing force can be calculated as,

$$F_{av} = \left(22.8\sqrt{\frac{c}{t}} + 5.7\right)\frac{\sigma_\circ t^2}{4\eta} \qquad (2)$$

where c is the flange length, and t is the thickness. The factor η, which ranges between 0.6–0.8, was introduced by Abramowicz (1983) to propose the effective crushing distance as the structure can not be crushed to a zero length. The characteristic flow stress $\sigma_\circ$ is typically taken as the average between the yield and ultimate stress of the material curve.

Experimental and Finite Element Methods

For the basic elements mentioned in the foregoing, a number of representative test results exist (e.g. Urban *et al.* (1999) and Simonsen (2000)). These results can be used as a benchmark in testing the performance of finite element formulations. For that purpose, an X–element resembling what is presented by Simonsen (2000) with a probable different height and material parameters has been selected for the analysis. The basic idea was at least to compare the failure mode predicted for a typical basic element.

The reference element has a height of 800mm, a flange width of 270mm, and a 15mm thickness. This yields c/t ratio equal to 18. The material was considered elastic–perfectly–plastic with properties $E = 2.1 \times 10^5$ MPa, $\sigma_Y = 300$ MPa, and $\nu = 0.3$. A small initial imperfection with a maximum amplitude of 1mm, based on the eigenproblem analysis, was introduced to trigger the buckling pattern.

Since the present implementation has not yet included the material fracture and contact algorithm, the basic element was compressed up to 100mm only. Thereafter, the deformations can not be simulated without fracture and contact models. Within the range of the analysis, however, the deformations show a very

Copyright © 2001 by ASME

fine agreement with the experimental observation as shown in Figure 15.

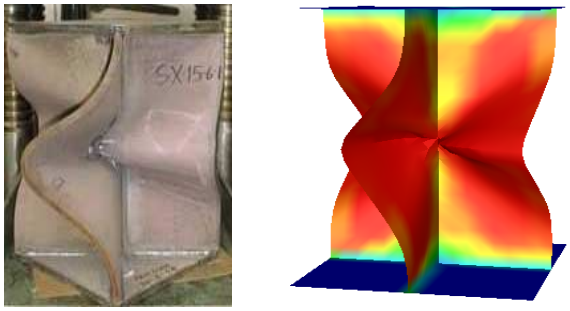

(a) Test; Simonsen (2000) (a) Simulation

Figure 15. AXIAL CRUSHING OF X–ELEMENT

In comparison with analytical models, the straight edge mechanism is clearly observed. The results of the finite element simulation are presented in Figure 16. The analytical value of the average crushing force as calculated by Equation 2 using $\eta = 0.8$ is presented in the figure as well.

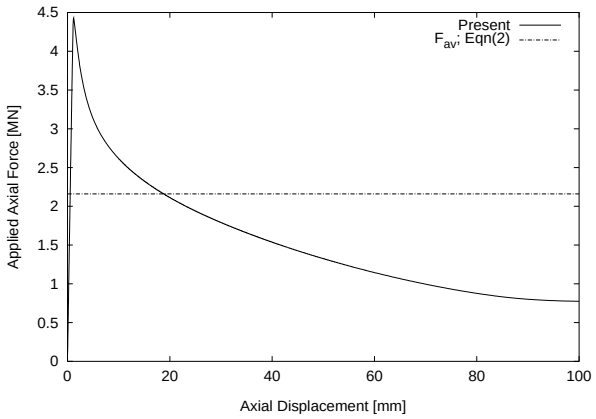

Figure 16. LOAD–SHORTENING CURVE FOR X–ELEMENT

CONCLUDING REMARKS

The performance of a simple non–linear finite element formulation has been verified by using different practical applications in ship and offshore structures. They include stiffened plates subjected to a combined axial compression and lateral pressure loads, shear collapse of an aluminum plate girder, and axial crushing of a cruciform. The simulations have been compared with the results from another detailed finite element program, experimental results, and predictions from design codes. With the presented results, it can be concluded that the present formulations perform equally well in relation to test results and other detailed finite element formulations.

ACKNOWLEDGMENT

The authors would like to extend their thanks to Langhelle and Eberg (1999) for the test results from an *aluminum plate girder*, and to Atle Johansen for carrying out its ABAQUS analysis.

REFERENCES

ABAQUS (1998). *General purpose finite element analysis program* (Version 5.8 ed.). USA: Hibbitt, Karlsson & Sorensen, Inc. User's Manual; Theoretical Manual.

ABRAMOWICZ, W. (1983). The effective crushing distance in axially compressed thin–walled metal columns. *Int. J. Impact Eng. 1*(3), 309–317.

AMDAHL, J. (1983). *Energy Absorption in Ship–Platform Impacts*. Ph. D. thesis, NTH, University of Trondhem, Norway.

DNV (1992). Buckling strength analysis. In *DnV Classification Note No. 30.1*. Høvik, Norway.

ECCS (1986). In P. DUBAS AND E. GEHRI (Eds.), *Behaviour and Design of Steel Plated Structures*. Swiss Federal Institute of Technology Zürich, CH–8093 Zürich, Switzerland: Applied Statics and Steel Structures. Publication No. 44.

EUROCODE-9 (1998, February). Design of aluminum structures [Part 1.1: General rules]. European Committee for Standardisation, Rue de Stassart 36, B–1050 Brussels. ENV 1999–1–1, CEN/TC 250/SC 9.

HÖGLUND, T. (1997). Shear buckling resistance of steel and aluminum plate girders. *Thin–Walled Structures 29*(1–4), 13–30.

KIERKEGAARD, H. (1993). *Ship Collision with Icebergs*. Ph. D. thesis, Technical University of Denmark, Denmark.

LANGHELLE, N. AND E. EBERG (1999). Ultimate strength testing of aluminum stressed skin structures at elevated temperatures. Report No. MT70 F99–398, Norwegian Marine Technology Research Institute, MARINTEK, SINTEF, Norway.

MOHAMMED, A. K., J. AMDAHL, AND B. SKALLERUD (2000). Collapse analysis of thin shell structures using a displacement–based constant stress–resultants curved element. Technical Report MK/R 146, Marine Structures Dept., Norwegian Univerisity of Science and Technology, NTNU, Norway.

Copyright © 2001 by ASME

MORLEY, L. S. D. (1971). The constant–moment plate–bending element. *J. Strain Anal. 6*(1), 20–24.

SIMONSEN, B. C. (2000). Personal homepage; Bo Cerup Simonsen's Research. Department of Naval Architecture and Offshore Engineering, Technical University of Denmark, DTU, Denmark. http://www.ish.dtu.dk/.

SKALLERUD, B. AND B. HAUGEN (1999). Collapse of thin shell structures – stress resultant plasticity modelling within a co–rotated ANDES finite element formulation. *Int. J. Numer. Meth. Engng 46*, 1961–1986.

URBAN, J., P. T. PEDERSEN, AND B. C. SIMONSEN (1999). Collision risk analysis for hsc. In *FAST'99*, pp. 181–194.

USFOS (1998). *A computer program for pregressive collapse analysis of steel offshore structures.* NTNU, Norway: SINTEF. User's Manual.

WANG, X. AND T. MOAN (1997, March). Ultimate strength analysis of stiffened panels in ships subjected to biaxial and lateral loading. *International Journal of Offshore and Polar Engineering 7*(1), 22–29.

Copyright © 2001 by ASME